

Damage prediction of long-period structures during subduction earthquakes Part2: Prediction of damage to high-rise buildings in the Osaka basin in future Nankai earthquakes

Yoshihisa NAKAGAWA¹, Katsuhiko KAMAE², Hidenori KAWABE³ and Kojiro IRIKURA⁴

1 Yasui Architects & Engineers Inc., Osaka, Japan

2 Professor, Research Reactor Institute, Kyoto University, Osaka, Japan

3 Assistant Professor, Research Reactor Institute, Kyoto University, Osaka, Japan

4 Professor, Disaster Prevention Research Center, Aichi Institute of Technology, Toyota, Japan

Email: ynakagwa@yasui-archi.co.jp, kamae@kuca.rri.kyoto-u.ac.jp, kawabe@rri.kyoto-u.ac.jp, irikura@geor.or.jp

ABSTRACT :

High-rise buildings in mega-cities such as Osaka and Nagoya in Japan have a high probability of damage due to strong long-period ground motions from a great subduction earthquake. We predict the damage potential of steel and reinforced concrete high-rise buildings and construct damage prediction maps for the Osaka basin using the long-period ground motions of future Nankai earthquakes predicted in our other paper (Part 1). In this study, a one mass model (an analytical model for the equivalent mass of one degree of freedom) is adopted due to the need for a great deal of earthquake response analysis. We have confirmed through both earthquake observation and analytical results regarding high-rise buildings that the displacement and earthquake input energy of high-rise buildings subjected to long-period ground motion can be approximately estimated by this simple model. Using damage prediction maps, we point out that the dynamic response of high-rise buildings exceeds the present seismic design criteria in wide areas inside the Osaka basin.

KEYWORDS: Long-period ground motion, Nankai earthquake, Osaka basin, High-rise building, One mass model, Damage prediction map

1. INTRODUCTION

If a great subduction earthquake with the magnitude 8 class (Tonankai/Nankai earthquake) occurs, there is an extremely high probability that large metropolitan areas such as Osaka and Nagoya, which are located on large sedimentary basins, will be struck by long-period ground motions typical of massive earthquakes. Long-period structures such as high-rise buildings, seismic isolated structures, large bridges and oil tanks are concentrated in mega-cities, and face unprecedented earthquake damage due to long-period ground motions.

In this research, we attempted to create damage maps limited to high-rise buildings (steel or reinforced concrete) using predicted long-period ground motions in the Osaka basin during a Nankai earthquake, given in Part 1. Since earthquake response analysis of buildings had to be conducted for an extremely high number of points (the Osaka basin being divided into a 1km mesh), we adopted the simplest one mass model as the analysis model.

First, we use actual observations to verify the validity of the assumption of the one mass model—i.e. that high-rise buildings vibrate almost entirely in the first mode in response to long-period ground motions. Next, we analyze responses to long-period ground motion of a frame model and one mass model with regard to a high-rise building model, and show that displacement and earthquake input energy of high-rise buildings can be approximately estimated using the one mass model. Based on the above, and using a response analysis method for the one mass model, we then create damage maps for steel and reinforced concrete high-rise buildings with respect to predicted long-period ground motions at each point of the Osaka basin during a Nankai earthquake.

2. EARTHQUAKE OBSERVATION RESULTS AND SIMULATION ANALYSIS FOR HIGH-RISE BUILDINGS

Here we introduce an observation where a high-rise building vibrated almost entirely in the first mode in response to actual long-period ground motions. In the Kii Hanto Nanto Oki earthquake on September 5, 2004 (magnitude 7.4), long-period ground motions were observed at various points in the Osaka basin. Fig. 1 shows the EW component of acceleration records at the B2 and top 23rd floors of a 116m high steel high-rise building located in the eastern Osaka basin. Major shaking of the top floor continued for over 2 minutes, and this was due to long-period ground motions with a predominant period close to 6 seconds, as indicated by the velocity response spectrum of acceleration records for the lowermost floor (B2 floor) in Fig. 2.

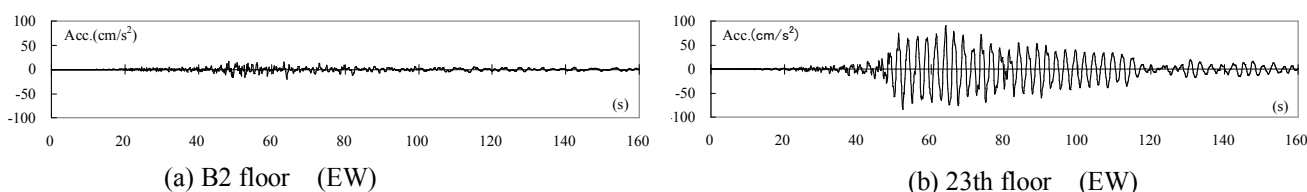


Figure 1 Acceleration records

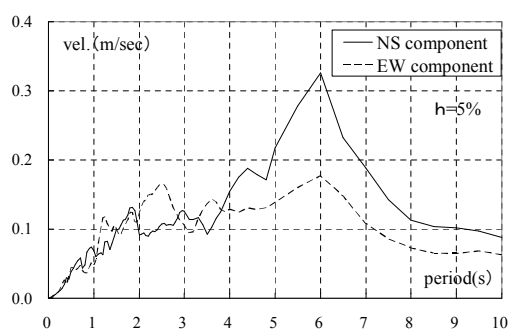


Figure 2 Velocity response spectrum of earthquake records at B2 floor

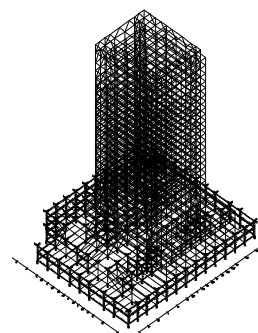


Figure 3 Frame model

Earthquake response analysis in the EW direction was conducted by replacing this building with the frame model shown in Fig. 3, and using the acceleration records as the input motion. Fig. 4 shows the acceleration time history at 23rd floor—both the observation records and analysis results using the frame model. The analysis results almost reproduce the observation records.

A one mass model with the same natural period (2.53 seconds) and damping ratio (1%) as the frame model was created, and a comparative analysis of the two models was done. If it is assumed that the building vibrates in the first mode, then the building displacement $\{D\}$ is determined according to Eqn.2.1 by the first participation vector $\{u_1\}$ and displacement of the one mass model \bar{D} . In this case, the displacement of the one mass model \bar{D} corresponds to displacement of the building position where the participation vector for the first mode is 1.0 (hereafter this is called “typical point displacement”).

$$\{D\} = \{u_1\} \bar{D} \quad (2.1)$$

Fig. 5 shows the displacement time history of the typical point (corresponding to the 17th floor) of the frame model in the EW direction, together with displacement \bar{D} of the one mass model. The one mass model exhibits almost the same values as the frame model. Next, the maximum displacement ${}_i D_{\max}$ and maximum story drift angle ${}_i R_{\max}$ of each floor were estimated by the following equation using the maximum displacement of the one mass model \bar{D}_{\max} , ${}_i u_1$ and story height H_i .

$${}_i D_{\max} = {}_i u_1 \bar{D}_{\max} \quad (2.2)$$

$${}_i R_{\max} = ({}_{i+1} D_{\max} - {}_i D_{\max}) / H_i \quad (2.3)$$

Fig. 6 shows results estimated using the one mass model together with results for the frame model, and there is a good correspondence between the two. The above results suggest that this building vibrated almost entirely in the first mode in response to long-period ground motion.

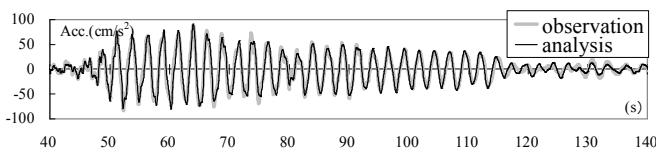


Figure.4 Observation records and analysis results using the frame model (Acceleration time history at 23rd floor)

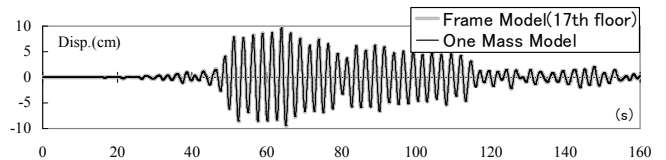
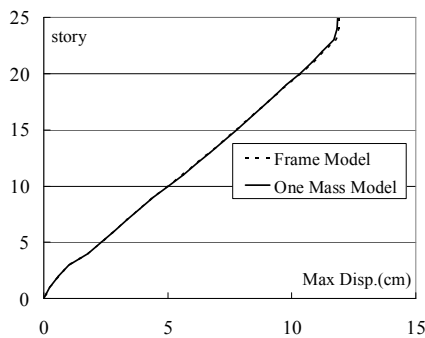
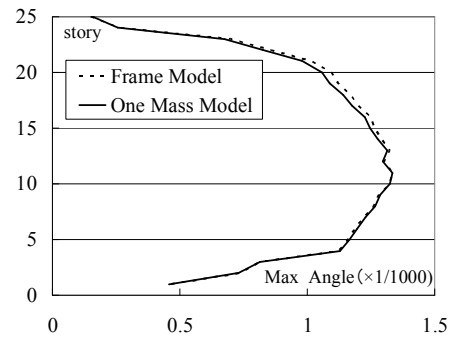


Figure.5 Displacement time history of both frame model (17th floor) and one mass model



(a) Maximum displacement



(b) Maximum story drift angle

Figure.6 Comparison of results using one mass model with results for frame model

3. DAMAGE INDICES OF HIGH-RISE BUILDING OBTAINED FROM RESPONSE PREDICTION USING THE ONE MASS MODEL

Generally when the first natural period of a buildings is in or less than the predominant period range of ground motion, the building will vibrate almost entirely in the first mode as shown in the preceding section. In particular, since we use the predicted long-period ground motions whose effective periods are longer than 2.5 seconds in this study, there is little possibility of higher modes being dominant even in high-rise buildings, given the assumption that the second natural period of buildings is nearly one third of the first natural period.

A building model was used to examine the degree to which response to long-period ground motions can be understood with a one mass model. The frame model for 82m high, 20 story steel building [2] shown in Fig. 7 was replaced with a one mass model, and a comparative analysis with the frame model was done in the Y direction (the first natural period 2.75 seconds). Fig. 8 shows the velocity response spectrum of the input motion, selected from the predicted ground motions in Part 1. With the one mass model, a building can be expressed with three parameters: the first natural period, yield base shear coefficient and damping ratio. We set the equivalent mass ratio for the first mode to 0.78, the damping ratio to 2%, and the yield base shear coefficient to 0.191. The hysteretic characteristic was set to be the normal bilinear model.

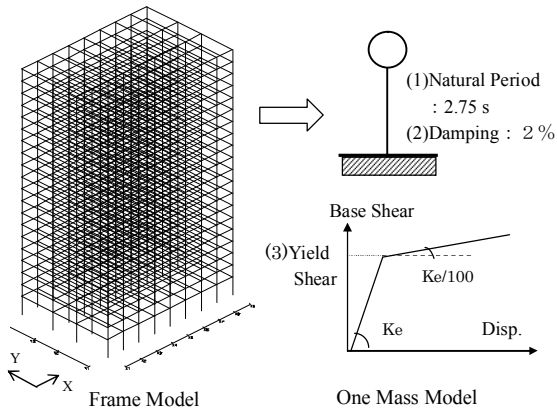


Figure.7 Frame model and one mass model for 20 story steel building

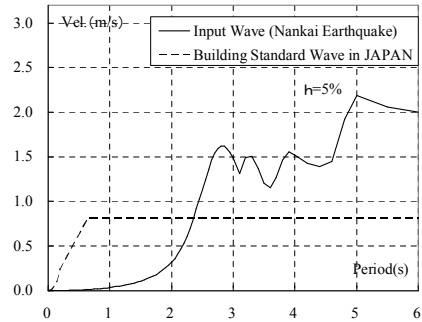


Figure.8 Velocity response spectrum of the input motion

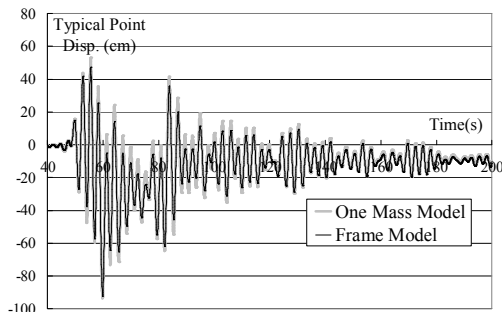


Figure.9 Displacement time history at building typical point

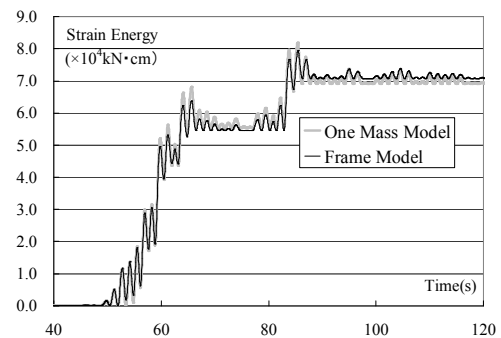


Figure.10 Time history of input energy contributing to damage (E_D)

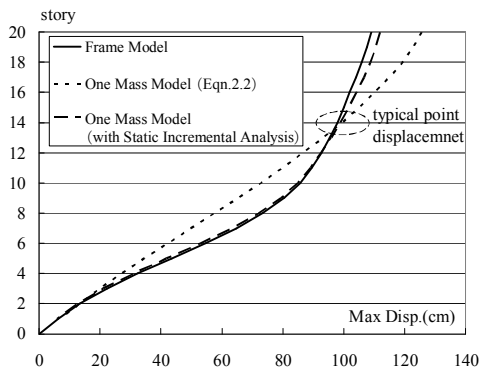


Figure.11 Maximum displacement

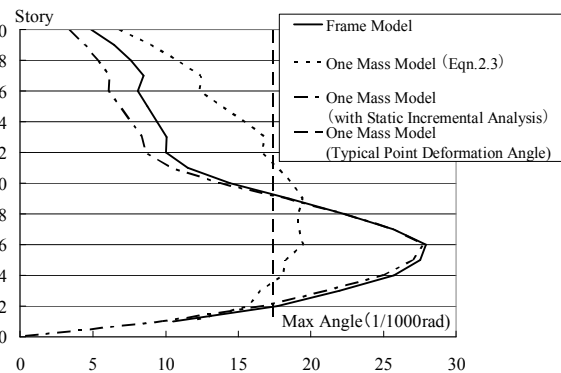


Figure.12 Maximum story drift angle

Figs. 9 and 10 show the time history of the typical point displacement and the total strain energy of beam and column members (hereafter called “input energy contributing to damage (E_D)”). For both response values, there is a good correspondence of the results for the one mass model and frame model. Figs. 11 and 12 show the maximum displacement and maximum story drift angle for each floor. The results for the one mass model, found using Eqn.2.2 and Eqn.2.3, are not greatly different from results for the frame model. This is because the displacement of each building floor depends on the relative relationship of the bearing strength distribution and external force distribution in the height direction of the building when the building enters the nonlinear domain. Thus, a static increment analysis was conducted taking the external force distribution as an Ai-distribution of the Japanese code, and the displacement and story drift angle for each floor, at the time when the typical point

displacement becomes the maximum displacement of the one mass model (\bar{D}_{max}), were shown in the same diagrams. There is a good correspondence with results for the frame model. Frame response results can be enough estimated even in the strongly nonlinear domain if static increment analysis is also used for analysis of the one mass model in this way. The maximum deformation angle of the building's typical point obtained from the one mass model \bar{r}_{max} (=maximum displacement of one mass model / building typical point height), is also indicated with a dotted line in Fig. 12. \bar{r}_{max} shows almost the average value of each story drift angle and the difference with the maximum story drift angle increases when deformation is concentrated at a specific floor.

In this paper, the following three characteristics are used as high-rise building damage indices obtained from above analysis of the one mass model.

- (a) Maximum building typical point displacement (\bar{D}_{max})
- (b) Maximum deformation angle of building typical point (\bar{r}_{max})
- (c) Velocity converted value of input energy contributing to damage E_D (V_D)

In the Japanese seismic design method based on energy balance, the design value V_D ($=\sqrt{2E_D/M}$) for buildings on medium class ground is required to be 165cm/s. Using this design method based on V_D , it is possible to calculate the necessary cumulative plastic deformation of beam and column members at each story [4].

4. DAMAGE PREDICTION FOR HIGH-RISE BUILDINGS IN THE OSAKA BASIN

4.1 Analysis model

Prediction of damage to steel and reinforced concrete high-rise buildings is done using the one mass model indicated below.

The hysteretic characteristic is set to the normal bilinear model for steel, and to the degrading trilinear model for reinforced concrete as shown in Fig. 13. Q_u in Fig. 13 is calculated using the yield base shear coefficient C_u given by Eqn.4.1, where C_1 is the base shear coefficient for the allowable stress design and is generally expressed by the first natural period T_1 . That is $C_1= 0.3/T_1$ for steel and $C_1= 0.18/ T_1$ for reinforced concrete [3]. Multiplier β is normally in the range 1.5–2.5. In the skeleton curve for reinforced concrete, we set Q_c/Q_u to 0.17 and K_y/K_e to 0.41, assuming a standard structure consisting of beam and column members.

$$C_u = \beta C_1 \tag{4.1}$$

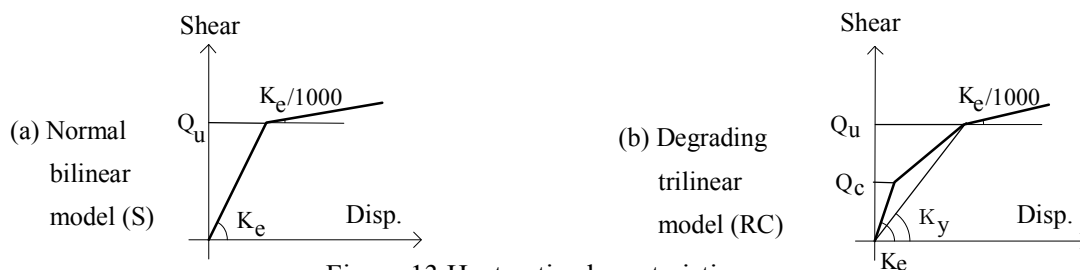


Figure.13 Hysteretic characteristics

The equivalent mass ratio is taken to be 0.78, assuming that the distribution of mass is uniform in height and the story drift angles of each floor are the same for external force with an A_i -distribution of the Japanese code. We use initial stiffness proportional damping with the first damping ratio set to 2% for steel, and instantaneous

stiffness proportional damping with the first damping ratio set to 3% for reinforced concrete. The height of the building typical point H_1 necessary for calculating \bar{R}_{\max} is found from the building height H and the participation factor for the first mode α ($= 1.37$), where H is generally expressed by T_1 , that is $H = T_1/0.026$ for steel and $H = T_1/0.019$ for reinforced concrete [3].

4.2 Damage map for high-rise buildings

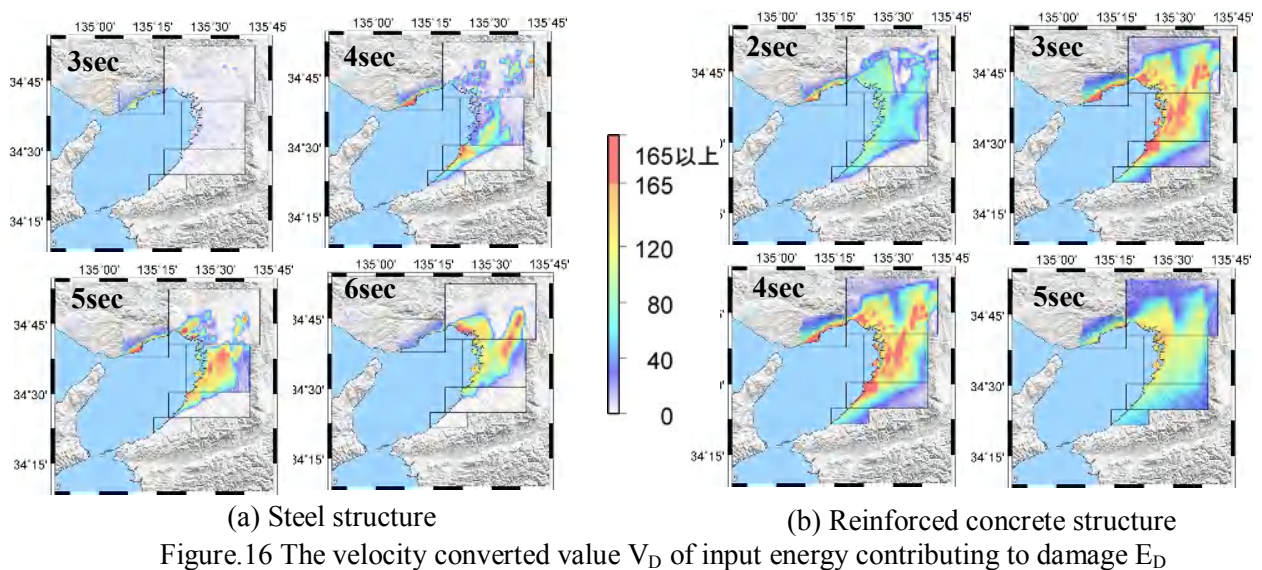
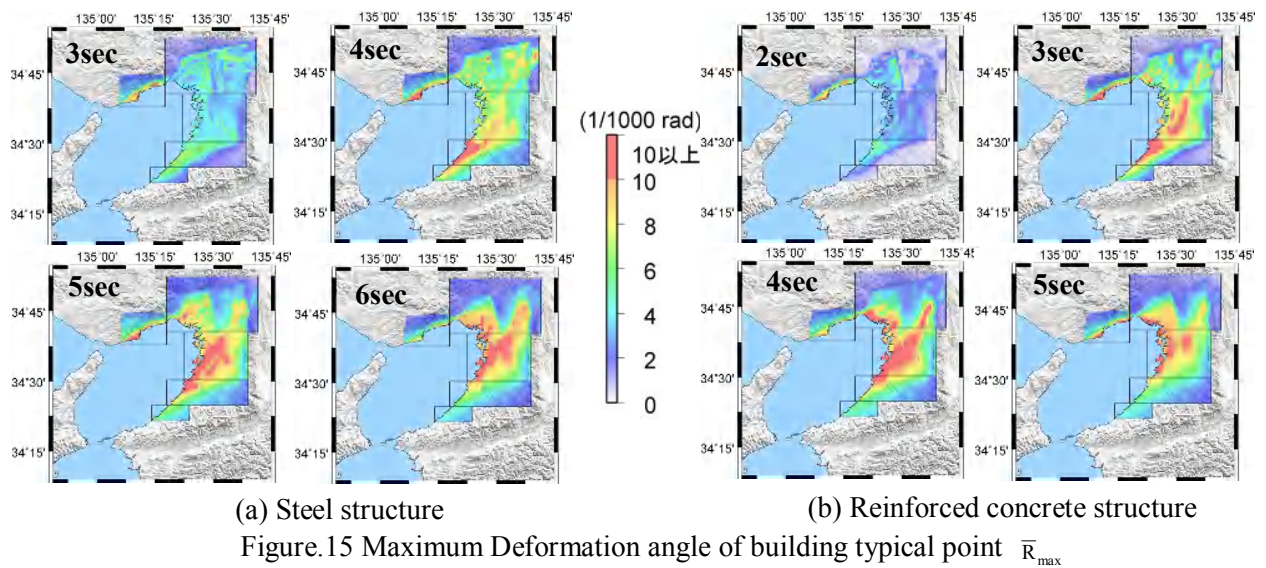
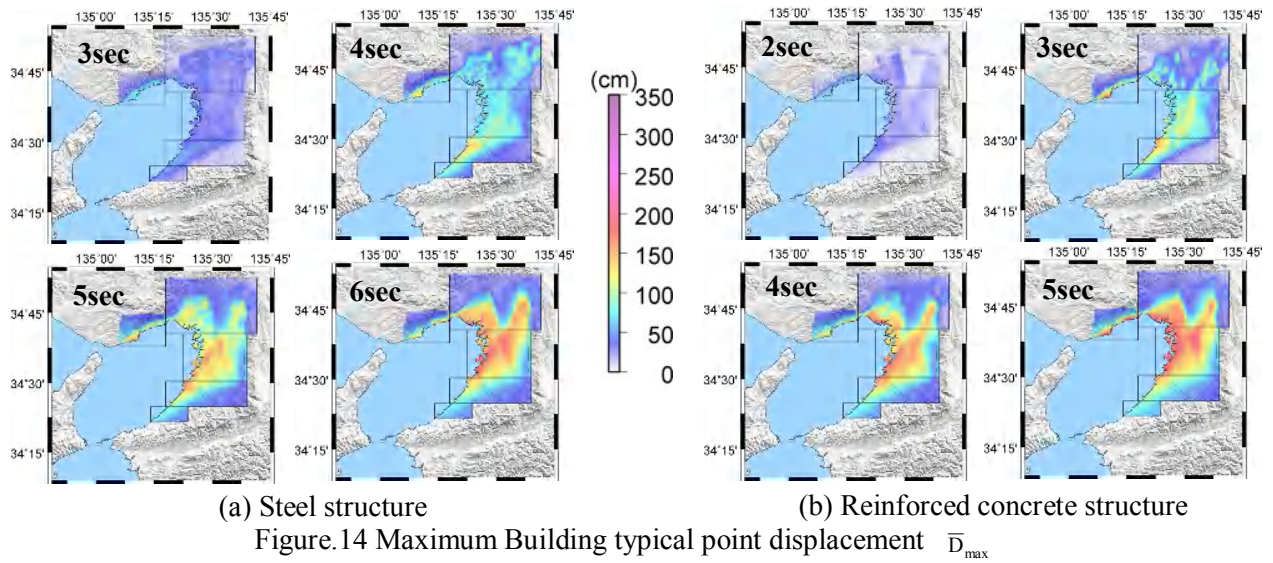
We conducted earthquake response analysis based on the one mass model for predicted ground motions at each point in the Osaka basin. Using the damage indices obtained from the above analysis, we constructed damage prediction map for high-rise buildings with natural periods of 3 to 6 seconds for steel and 2 to 5 seconds for reinforced concrete.

Figs. 14–16 show damage maps for \bar{D}_{\max} , \bar{R}_{\max} and V_D of steel and reinforced concrete high-rise buildings with one second increment of natural periods. We used ground motions for the NS component whose maximum velocity is larger than the EW component at most points as shown in Part 1, and β in Eqn.4.1 is 2.0, which is an average value of building bearing strength. The following points can be noted from these earthquake damage maps.

- (1) There are many regions where the maximum deformation angle of the typical point \bar{R}_{\max} , which indicates the average value of the story drift angles for each story, exceeds the design criteria (1/100) for the story drift angle of a high-rise building, and regions where the velocity converted value V_D of the input energy contributing to damage exceeds the design criteria (165cm/s) for buildings on medium class ground. If there are high-rise buildings with the pertinent natural period in these regions, it would be desirable to conduct more detailed studies in the future.
- (2) Regions where there is large deformation of steel high-rise buildings are: the Kobe coast for buildings with a natural period of 3 seconds, the Kobe coast and southern Osaka for buildings with a period of 4 seconds, and almost everywhere except southern Osaka for buildings with a period of 5 or 6 seconds. Large earthquake energy is input over a wide range of the Osaka basin particularly for buildings with a period of 5 or 6 seconds.
- (3) Regions where there is large deformation of reinforced concrete high-rise buildings are: the Kobe coast for buildings with a natural period of 2 seconds, the Kobe coast and the central/southern Osaka basin for buildings with a period of 3 seconds, and almost everywhere except southern Osaka for buildings with a period of 4 or 5 seconds. Large earthquake energy is input over a wide range of the Osaka basin for buildings with a period of 3 or 4 seconds. Reinforced concrete buildings enter the nonlinear domain quickly due to cracking of concrete, and thus input energy contributing to damage is greater than for steel buildings.

5. CONCLUSION

Focusing on the Osaka basin, where there is a high probability of being struck by strong long-period ground motions in the case of a potential Nankai earthquake (M8.4), we have created damage maps for steel and reinforced concrete high-rise buildings, and shown that story drift angles and earthquake energy inputs exceeding the present design criteria can potentially occur over a wide range, depending on the building natural period band. This applies in particular to steel buildings with a first natural period of 5 to 6 seconds, and reinforced concrete buildings with a period of 4 to 5 seconds. With the ground motion for design of high-rise buildings in current Japanese building code, the characteristics of the subsurface ground are taken into account as site characteristics, but there is no consideration of the characteristics of deep ground structures, which are closely related to the period band (longer than 2.5 seconds) of the predicted long-period ground motions used in



this research. In the Osaka basin, where dominance in a longer period band is predicted in a Nankai earthquake or other massive earthquake, there is a need to examine the seismic safety of high-rise buildings using predicted ground motions which also take into account deep ground structures.

When predicting damage over a wide area to long-period structures due to long-period ground motions, the technique based on a one mass model given here is useful for easily developing an understanding of the general situation. If some basic information regarding an individual building is known—i.e. building position, structural type, natural period, yield base shear coefficient—then it is possible to roughly understand the building's average story drift angle and input energy contributing to damage from the damage map. It is also possible to estimate the maximum story drift angle of each floor by conducting static increment analysis of the building up to the index \bar{D}_{\max} . The necessary cumulative plastic deformation of beam and column members can be approximately estimated from the index V_D by using the calculation technique based on energy balance.

The uncertainty of the characteristics of buildings and predicted ground motions cannot be denied in predicting earthquake damage to buildings. The damage maps presented here apply to high-rise buildings having average restoring force characteristics and damping characteristics, and the assumed Nankai earthquake is based on a single scenario. Damage maps based on a one mass model can be created comparatively easily, and thus in the future we plan to apply this technique to different characteristics of buildings and multiple scenario earthquakes, and examine the resulting effects. Also, this study focused on long-period ground motions of 2.5 seconds or longer, and future studies will need to look at a wider band of predicted ground motions, and take into account the higher order modes of high-rise buildings.

ACKNOWLEDGEMENTS

This research was conducted based on a Grant-in-Aid for Scientific Research, Basic Research (B) (Grant no.: 17310108). In preparing this manuscript, valuable comments were received from the grant recipient and other collaborators, and the authors would like to express their gratitude.

REFERENCES

1. Comartin, C., R. Niewiarowski and C. Rojahn (1996). Chapter 8 Nonlinear static analysis procedures, ATC-40 Seismic evaluation and retrofit of concrete buildings Volume 1, Applied Technology Council.
2. Sekiya, E., H. Mori, T. Ohbuchi, K. Yoshie, H. Hara, F. Arita., Y. Takeuchi, I. Y. Saito, M. Ishii, and K. Kasai (2004). Details of 4-, 10-, & 2- story theme structure used for passive control design examples, *Passive Control Symposium 2004*, 263-278.
3. Kimura, U., S. Ichimura, T. Fukushima, and T. Teramoto (2000). Study on the mechanical feature of high-rise building, *Summaries of technical papers of Annual Meeting AIJ*, Structures 3, 865-866.
4. Hasegawa, T., I. Nishiyama, A. Mukai, T. Ishihara and H. Kamura (2004). Seismic response prediction of steel frames with hysteretic dampers based on energy balance, *Journal of structural and construction engineering, AIJ*, No582, 147-154.
5. Kawabe, H., K. Kamae and K. Irikura (2007). Damage prediction of long-period structures during great subduction earthquakes Part1: Long-period ground motion prediction in the Osaka basin for the future Nankai Earthquake, *Summaries of technical papers of Annual Meeting AIJ*, Structures 2, 415-416.
6. Nakagawa, Y., K. Irikura, K. Kamae and H. Kawabe (2007). Damage prediction of long-period structures during great subduction earthquakes Part2: Damage prediction map of steel high-rise buildings in the Osaka basin for the future Nankai Earthquake, *Summaries of technical papers of Annual Meeting AIJ*, Structures 2, 417-418.